Highlighting research from the group of Dr Leonardo Chiappisi of the Partnership for Soft Condensed Matter at the Institut Laue–Langevin in Grenoble in collaboration with the University of Palermo.

Hierarchical assembly of pH-responsive surfactant–cyclodextrin complexes

We present the hierarchical assembly of cyclodextrins with pH-responsive surfactant into highly structured supramolecular assemblies, with typical length scales spanning several orders of magnitude. The spontaneously formed inclusion complexes crystallize in ordered lattices, which further organize into multilayered cylinders of several micrometers length.

As featured in:

Soft Matter

ROYAL SOCIETY OF CHEMISTRY

See Leonardo Chiappisi *et al.*,
Soft Matter, 2022, **18**, 6529.

ROYAL SOCIETY
OF **CHEMISTRY**

rsc.li/soft-matter-journal

Check for updates

Hierarchical assembly of pH-responsive surfactant–cyclodextrin complexes†

Larissa dos Santos Silva Araújo,[ab] Leah Watson,[b] Daouda A. K. Traore, [ID][bc] Giuseppe Lazzara [ID][a] and Leonardo Chiappisi [ID] *[b]

In this work, the inclusion complexes of alkyl ethoxy carboxylates with α-cyclodextrin (αCD) and β-cyclodextrin (βCD) were investigated. The thermodynamics of the complexation process was probed by isothermal titration calorimetry (ITC) and volumetry as a function of the degree of ionization of the surfactant. The complexation process was shown to be an enthalpically driven pH-independent process. For both types of cyclodextrins, the complexes were found to spontaneously self-assemble into highly-ordered supramolecular aggregates probed by small-angle neutron scattering and electron and optical microscopy. Herein, we report the formation of thin platelets for nonionized surfactant systems and equally spaced multilayered hollow cylinders for ionized systems in a hierarchical self-assembly process. In addition, the analysis allowed unveiling the effect of the number of ethylene oxides in the surfactants and the CD cavity size on the morphology of the aggregates. Finally, this study also highlights the importance of examining the tuning parameters' influence on the short and long-range interactions involved in the control of the assembly process.

1 Introduction

Cyclodextrins (CD) are a class of cyclic oligosaccharides formed through α(1–4) ether linkage glucopyranose units. The most common ones, α, β, and γCD are respectively formed by six, seven, and eight glucopyranose units. The truncated cone shape structure with a hydrophilic outer surface and a hydrophobic cavity, ranging from 5 to 8 Å, provide unique physicochemical properties to CDs, particularly the ability to form host–guest complexes.[1] The hydrophobic cavity, hydrophilic rims, the electron density, and the presence of the high-energy water in the cavity drive the assembly with a large range of different molecules, such as drugs,[2] polymers,[3–5] and surfactants,[6,7] affecting their properties.[8]

In turn, surfactant molecules and amphiphilic polymers self-assemble in aqueous solutions above a defined concentration. Admixing cyclodextrins to self-assembled copolymer aggregates generally leads to the disruption of the micelles when the hydrophobic moieties are complexed or to the

formation of decorated micelles, when the hydrophilic part of the polymer is threaded.[9–11]

In contrast to the CD-induced disassembly of copolymer aggregates, highly ordered supramolecular complexes are found in mixtures with low molecular weight surfactants, such as sodium dodecyl sulfate,[12] polyoxyethylene sorbitol esters[13] and dodecyltrimethylammonium bromide.[14] In these mixtures, vesicles,[12,13] hydrogels,[15] fibers,[16] tubular and lamellar[17] structures have been reported, depending on the concentration, temperature, and mixing ratio. Such hierarchical assembly process is mainly governed by the intermolecular interactions between the cyclodextrins and the repulsive forces provided by the guest molecules. In addition, the importance of the water-mediated hydrogen-bonding network in the inclusion complexes' self-organization into ordered structures has been proven.[14,18,19] Up to now, however, systematic structural studies have been performed with either ionic or nonionic surfactant complexes.

In contrast, this work deals with the investigation of inclusion complexes between α and βCD with the weakly anionic alkyl ethylene oxide carboxylic acids (AECs), whose carboxylic headgroup exhibits a pK_a of approx. 4.[20] The presence of terminal carboxylic group and ethylene oxide units (EO) in their molecules provide them pH and temperature responsiveness, respectively.[20]

Previous studies have shown that the nature of the surfactant has remarkably little impact on the supramolecular assembly of the inclusion complexes into bilayered structures, which is mainly governed by CD–CD interactions. In contrast, electrostatic

[a] *Dipartimento di Fisica e Chimica, Università degli Studi di Palermo, Viale delle Scienze pad 17, 90128, Palermo, Italy*

[b] *Institut Max von Laue – Paul Langevin, 71 Avenue des Martyrs, 38042, Grenoble, France. E-mail: chiappisil@ill.eu*

[c] *School of Life Sciences, Keele University, Staffordshire ST5 5BG, UK*

interactions determine the spacing and the ordering in multi-layered aggregates.[21] The aim of this work is to systematically investigate the effect of the surfactant charge on the inclusion complex formation and self-assembly properties.

The use of a pH-responsive surfactant allows us, on the one hand, to systematically investigate the effect of the charge density on the supramolecular assembly of the complexes, and on the other hand, is expected to provide pH sensitivity to mixtures for applications in the field of cosmetics, drug delivery, and food science.[8]

In detail, we investigated the thermodynamics of the inclusion complexes formation between two alkyl ether carboxylic acids: the pentaoxyethylene dodecyl carboxylic acid ($C_{12}E_5Ac$) and the decacyloxyethylene dodecyl carboxylic acid ($C_{12}E_{10}Ac$), with αCD and βCD by isothermal titration calorimetry (ITC) and densitometry. The structural characterization of the supramolecular aggregates arising from their assembly was conducted by small-angle neutron scattering (SANS) and optical and electron microscopy. We probed the effect of the chemical architechture of surfactant and CD, as well as the mixing ratio of the components ($Y = [CD]/[S]$), total concentration, surfactant degree of ionization – defined as the sodium hydroxide and surfactant molar ratio ($\alpha = [NaOH]/[S_{tot}]$) – on the formation of the inclusion complexes and the morphology of the structures arising from their assembly.

To the best of our knowledge, this study provides the first evidence of the pH-modulated assembly of the surfactant-CD inclusion complexes in different length scales, from the complexation to the assembly in higher magnitude supramolecular aggregates. Herein, the results presented open many possibilities for investigating the role of electrostatic interactions in the self-assembly process into supramolecular aggregates.

2 Experimental section

2.1 Materials

Pentaoxyethylene dodecyl carboxylic acid ($C_{12}E_5Ac$) and decacyloxyethylene dodecyl carboxylic acid ($C_{12}E_{10}Ac$) are technical surfactants provided by KAO chemicals under the trade names AKYPO RLM45CA (444 g mol^{-1}, 92% purity) and AKYPO RLM100 (686 g mol^{-1}, 90% purity), with 7.3 and 9.8 wt% water content, respectively, according to the producer. According to previous studies,[20,22] the hydrophobic part of the surfactants is a mixture (C_{12}, C_{14}, C_{16}) in approx. ratio 2 : 1 : 0.25. The ethylene oxide units (EO) are Gaussian distributed over a mean of 5 and 9 averaged distributions for AKYPO RLM45CA and AKYPO RLM100. αCD and βCD were purchased from TCI Europe. The water content of the cyclodextrins was determined from thermogravimetry, and it is 10.1 and 11.5 wt% for α and βCD, respectively. Sodium hydroxide (Fluka, puriss) was used to adjust the pH of the solutions. The water content in the reagents was considered for sample preparation. All chemicals mentioned were used as received. Solutions were prepared using Milli-Q water. Heavy water (D content > 99.8%) from

Eurisotop (Gif-sur-Yvette, France) was used for the small-angle neutron scattering experiments.

2.2 Sample preparation

The samples were prepared by adding the cyclodextrin solution to the surfactant solution to obtain the desired concentrations in the samples at ambient conditions. Samples were allowed to stabilize for 24 hours.

2.3 Molecular weight determination

The molecular weight of the aggregates (M_w) was calculated using eqn (1) using the determined transmission values T recorded at wavelength $\lambda = 633$ nm on a Varian Cary 50 UV-vis spectrometer (PSCM, Grenoble, France). After the measurement, the samples were heated for one hour at 70 °C and let to cool down overnight before another set of measurements. The measurements were repeated after seven days.

$$M_w = -\frac{\ln T}{c \cdot l \cdot H_0} \tag{1}$$

with, T being the transmittance of the sample, l is the thickness of the cuvette, c, the total concentration of surfactant and cyclodextrin and, $H^0 = 32\pi^3 n_0^2 (dn/dc)^2/(3N_A\lambda^4)$, in which $n_0 = 1.33$, is the refractive index of the solvent, λ is the wavelength of light used, N_A is the Avogadro constant $dn/dc \approx 0.120$ cm^3 g^{-1} and $dn/dc \approx 0.186$ cm^3 g^{-1} as refractive index increments of surfactant and CD, respectively.[23,24]

The concentration of the surfactant was kept constant at 7×10^{-3} mol kg^{-1} and 4×10^{-3} mol kg^{-1} for αCD and βCD systems, respectively.

2.4 Densitometry

The apparent molar volume of the cyclodextrin in surfactant solution was determined using an Anton Paar oscillating tube density meter DMA 5000M (PSCM, Grenoble, France).

$$V_\Phi = \frac{M_w}{\rho} - \frac{10^3(\rho - \rho_0)}{m \cdot \rho \cdot \rho_0} \tag{2}$$

where, M_w, m, ρ, and ρ_0 are the molecular weight (g mol^{-1}) and the molality of the CD (mol kg^{-1}), and the density of the CD/surfactant solution (g cm^{-3}) and the corresponding surfactant solution (g cm^{-3}), respectively.

The volume of transfer of cyclodextrin from water to the surfactant solutions (ΔV^{CD}) was calculated by the difference between the apparent molar volume of the cyclodextrin in the samples ($V_{\Phi,sample}^{CD}$) and in water ($V_{\Phi,water}^{CD}$), i.e., at zero surfactant concentration by

$$\Delta V^{CD} = V_{\Phi,sample}^{CD} - V_{\Phi,water}^{CD} \tag{3}$$

2.5 Isothermal titration calorimetry

Experiments were conducted in a Microcal VP-ITC (IBS, Grenoble, France) at 25 °C. Aliquots of the cyclodextrin solution were added to the reaction cell containing the surfactant solution. Measurements were carried out at pH 3, 4, and 5 in triplicate. Averaged ITC data of triplicates were analyzed.

2.6 Small-angle neutron scattering (SANS)

SANS patterns were recorded using 1 mm path quartz cells at $D11$,[25] and $D22$[26] at the Institut Laue–Langevin (Grenoble, France). At $D11$, with the wavelength of 6 Å ($\lambda/\Delta\lambda$ = 10%), three sample-detector configurations were used 1.4, 8 and 39 m and collimation of 5.5, 8 and 40.5 m, covering a q-range from 0.01 to 6 nm^{-1}, where $q = 4\pi\sin(\theta/2)/\lambda$. At $D22$, with a two ^{3}He detector setup, one fixed detector at 1.4 m sample-to-detector distance and, the second, used in two sample-to-detectors centre distance of 5.6 and 17.6 m distance with corresponding collimation of 5.6 and 17.6 m, covering a total q-range of 0.03 to 6 nm^{-1}.

2.7 Optical microscopy

For the observation of the aggregates' morphology, the samples were directly placed over a glass plate and examined using a BX61 Olympus (PSCM, Grenoble, France), in differential interference contrast (DIC) mode, and a Zeiss standard Polarized light Microscope (Olympus BX50) equipped with a camera CMOS.

2.8 Electron microscopy

For TEM, a small drop of sample was placed onto a copper TEM grid, and the excess was removed with filter paper. The sample was not stained. TEM observations were performed in a Tecnai12 Microscope operating at 120 kV (IBS, Grenoble, France). For Cryo-EM analysis, a few microliters of samples were placed onto a copper TEM grid, and the excess was removed using filter paper. Vitrification was conducted using a Vitrobot Mark IV (Thermo-Fisher Scientific) set to 10 °C and 100% humidity by plunging into liquid ethane. Image acquisition was performed on a FEI Talos Arctica TEM (200 kV).

3 Results and discussion

3.1 Phase behaviour

The goal of this study is to probe the interaction between the CDs and alkyl ether carboxylates and to explore the assembly behaviour as a function of the charge density α of the surfactant – defined as the ratio of added sodium hydroxide and surfactant molecules – and as a function of the surfactant/CD polymer ratio Y. Herewith, α defines the degree of ionization of the surfactant and the mixing ratio Y is a key parameter which controls the stoichiometry between host and guest. Experiments are performed at surfactant concentration approx. three orders of magnitude above the cmc, thus the interaction between CDs and micellized surfactant are being probed.

The assembly of the inclusion complexes between surfactants and cyclodextrins is characterized by the increase of the turbidity followed, in some cases, by the precipitation of white solids, as observed for other nonionic and ionic surfactants.[13,17] Aiming to understand the behaviour of those systems observing the mentioned parameters, the phase behaviour of the mixtures of each surfactant with αCD and βCD was investigated before and after being heated up to 70 °C for one hour and cooled at room temperature for 24 hours.
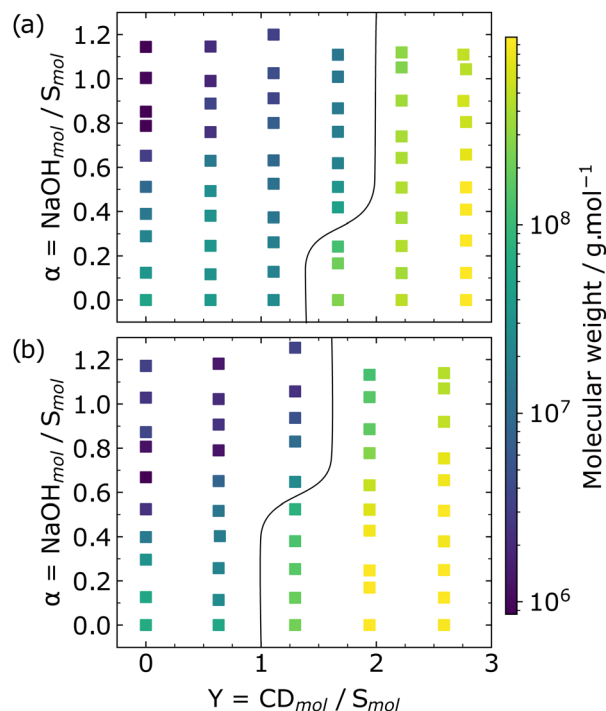

Fig. 1 Phase behaviour of $C_{12}E_5Ac$-αCD before heating (A) and after heating (B). The solid line separates the one-phase (left) and the two phase (right) regions. All data are recorded at room temperature. Phase diagrams of the $C_{12}E_5Ac$-βCD, $C_{12}E_{10}Ac$-αCD and $C_{12}E_{10}Ac$-βCD systems can be found in the ESI† (S2).

Macroscopically, we observed that all the systems examined presented increased turbidity from a particular value of Y, and clearer solutions were obtained with the increase of the pH, *i.e.* increasing the degree of ionization of the surfactant. The average molecular weight of each sample calculated by eqn (1) provides quantitative support to the macroscopic observations.

The phase boundaries were assigned at the phase diagrams for observations of $C_{12}E_5Ac$-αCD complexes before and after heating and cooling are presented in Fig. 1 (see ESI† for the phase diagrams of $C_{12}E_5Ac$-βCD (Fig. S2, ESI†) and $C_{12}E_{10}Ac$ systems (Fig. S3, ESI†). Heating followed by slow cooling of the samples shifts the phase boundaries towards greater values of Y regardless the CD type. This shift indicates the presence of colloidally stable aggregates, which can be an interesting feature for systems in different areas of applications. By increasing the ionization of the surfactant, the stabilization of the aggregates due to the electrostatic repulsion results in the decrease of the M_w observed. In order to gain insights into the inclusion complexes formation, calorimetric and volumetric studies were performed to provide information about the thermodynamics of the process.

3.1.1 Isothermal titration calorimetry (ITC). ITC allows provides a direct measurement of the interaction heat between the CD and surfactant, making the determination of binding constant (K), enthalpy change (ΔH) and stoichiometry (n) possible. Titration curves of the four surfactant–CD systems at pH 3, 4 and 5 are depicted in Fig. 2.
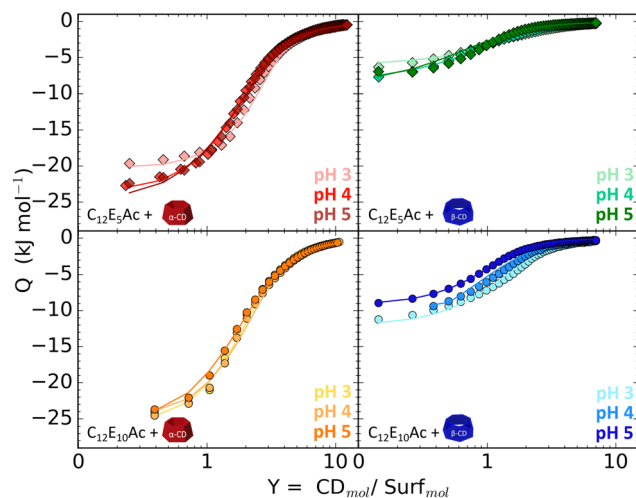
Fig. 2 Calorimetric curves for titration of $C_{12}E_5Ac$ ($\diamond$) and $C_{12}E_{10}Ac$ ($\bigcirc$) with αCD (left) and βCD (right) at pH 3, 4 and 5, 25 °C. Solid lines are the fits by the one-to-one binding model, which data is depicted in Fig. 3.

The heat of dilution of each component was measured, and the demicellization heat of the surfactants was assessed, both confirmed to be negligible. The heats of interaction were fitted
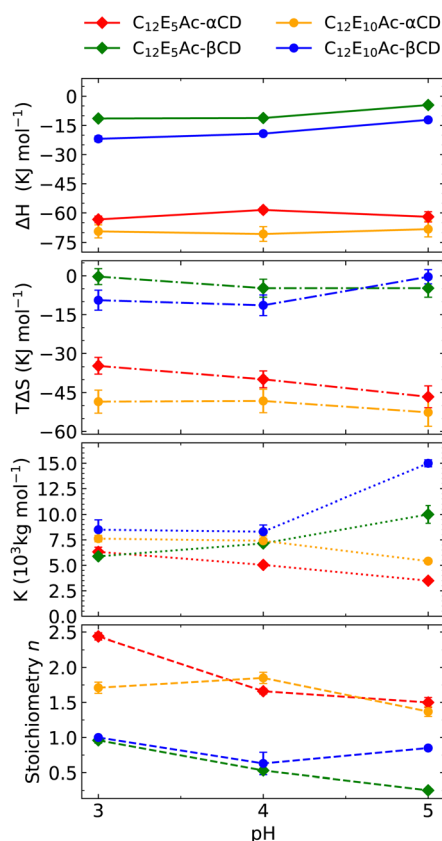

Fig. 3 Thermodynamic parameters obtained by ITC for the formation of host–guest complexes between AECs and cyclodextrins at 25 °C: ΔH (– solid line), $T\Delta S$ (·—·), binding constant 'K' (· ·) and stoichiometry (– –). The stoichiometry n is given in CD per surfactant molecule, while ΔS and ΔH are given in Joule per mole of surfactant.

assuming the presence of n independent and equal binding sites per surfactant molecule.

From the fit, the binding constant K, the stoichiometry n, i.e. the number of CD per surfactant, and the enthalpy of inclusion ΔH obtained allowed the calculation of the binding free energy and entropy change using the eqn (4) and (5), using a dimensionless K for the calculations.

$$\Delta G^\circ = -RT \ln K \tag{4}$$

$$\Delta S = \frac{\Delta H - \Delta G^\circ}{T} \tag{5}$$

The obtained thermodynamic quantities, i.e., ΔH, ΔG, ΔS, are calculated per mole of surfactant and are given in Fig. 3. The data indicates the spontaneous formation of the host–guest complexes ($\Delta G^\circ < 0$) for all the systems evaluated. Both ΔH and $T\Delta S$ present negative values. In all the cases, the lowest enthalpic change value provides a greater contribution to the complexation process, characterizing it as an enthalpically-driven mechanism.

The differences in the entropic contributions of α and β-cyclodextrins are mostly associated with the water structure inside the CD cavity, which is directly related to the CD size. In the cavity, the conformation of the glucopyranose units limits their hydrogen-bonding network, which provides more conformational freedom. In addition, the hydroxyl groups present at the CD rim can also be incorporated into the water network.[27] The full reestablishment of the hydrogen bonding network of those molecules is achieved with their release to the bulk, adding a contribution to the decrease in enthalpy. Oppositely to the straightforward assumption of the scaling of these effects with the increase of the cavity size, the heat capacity of the water within βCD is closer to the liquid water than the within the αCD,[28] resulting from structural differences between them. Hence, due to the different density of the water molecules inside the cavities, a greater enthalpic and unfavored entropic contribution for the inclusion complexation with αCD can be observed.

From the graphs, it is possible to notice that the main energetic features are related to the type of cyclodextrin. The most noticeable difference between the αCD and βCD systems curves is the magnitude of the enthalpy and entropy binding, whereas a small effect of the EO number is evidenced by the difference in the systems with $C_{12}E_5Ac$ and $C_{12}E_{10}Ac$ for both CD types. Minor effects of pH were observed, indicating that the terminal carboxylic group is not included in the CD cavity. Moreover, due to the very different hydration of the EO units in the ionized and non-ionized form of the surfactant, it is likely that the binding involves the hydrophobic part of the surfactant only. It is noteworthy that the experiments are carried out well above the cmc of the surfactant, and thus the interaction of the CDs with the surfactant micelles is also probed. In addition, the great affinity between host and guest is verified by the high binding constant values.

Similar thermodynamic/energetic behaviour had been reported in the literature for fatty acids and non ionic
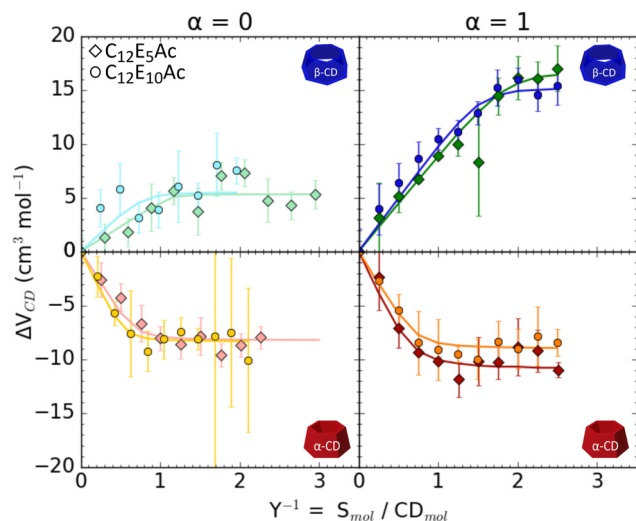
Fig. 4 Volume of transfer (ΔV^{CD}) of α-cyclodextrin and β-cyclodextrin from water to aqueous solution of $C_{12}E_5Ac$ (◇) and $C_{12}E_{10}Ac$ (○) as function of surfactant–CD ratio. Solid lines are the best fit according to eqn (6).

surfactants containing EO units. For the fatty acids containing 11 and 13 carbons in the alkyl chain, the inclusion complexation was also enthalpically driven and present $\Delta G < 0$, slightly more negative for the longer alkyl chain.[29] Inclusion complexes of βCD with Brij surfactants, also above the cmc, and Triton-100, in concentrations below the cmc, presented similar thermodynamic behaviour. However, the encapsulation of both hydrophobic and hydrophilic moieties was observed for the former, while for the latter, only the encapsulation of the hydrophobic moiety was reported.[30,31]

3.1.2 Volumetry. The inclusion complexation mechanism of a guest into the CD cavity is related to the spatial/geometric and energetic aspects *via* non-covalent interactions, such as electrostatic, van der Waals, hydrophobic, charge-transfer interactions and hydrogen bonding.[32] Thus, the volumetric study of CD complexes can provide a good insight into the solvation behaviour, and a better understanding of the phenomena and the interactions involved in the formation of such complexes.[33]

The volumes of transfer of αCD and βCD from water to the aqueous surfactant solution as a function of the S/CD molar ratio in the nonionic form ($\alpha = 0$) and in the completely ionized form ($\alpha = 1$) are presented in Fig. 4. The V_Φ determined for both CDs, 604.1 ± 0.1 and 706.7 ± 0.1 cm^3 mol^{-1}, for αCD and βCD, respectively, are in accordance with the literature[34,35] and were used in the calculation of the volumes of transfer.

The volumes of transfers are reported in Fig. 4, and it can be seen that: (i) the number of EO units of the surfactant has no effect on the volume of transfer; (ii) the volumes of complexation are positive for βCD and negative for αCD, as a consequence of the different water density within the cavity prior to complexation;[36,37] the charge of the surfactant has no effect for the complexation with αCD. The data can also be quantitatively
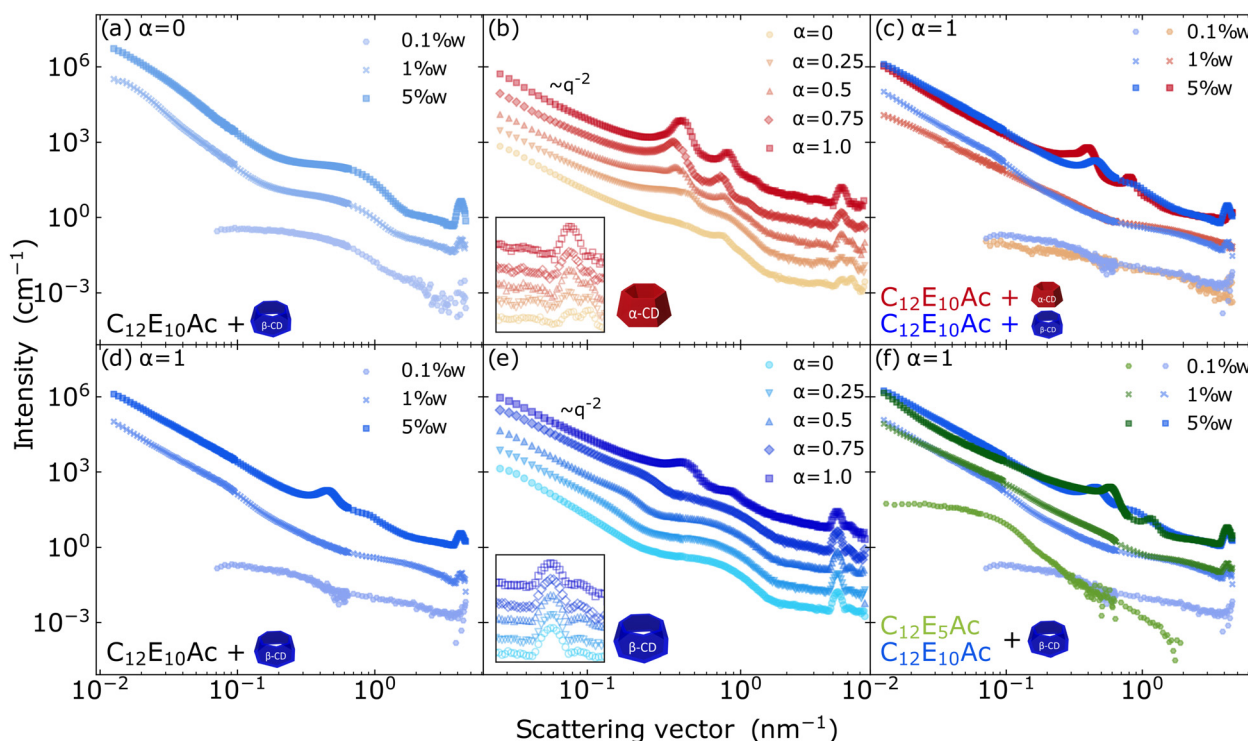

Fig. 5 At ratio CD/surfactant = 2, different concentrations of the $C_{12}E_{10}Ac$ with βCD at (a) $\alpha = 0$ (nonionized), (d) $\alpha = 1$ (ionized). Different degree of ionization (α) scattering profile curves of $C_{12}E_{10}Ac$ with αCD (b) and βCD (e). (c) Ionized surfactant with αCD (red) and βCD (blue). (f) Comparison of βCD with ionized $C_{12}E_5Ac$ (green) and $C_{12}E_{10}Ac$ (blue) at different surfactant concentrations. Curves are scaled by successive factors of 7 for readability. Measurements of a, c, d and f were performed on D11 and b and e on D22 at ILL.

interpreted. As performed for the ITC modelling, the one-to-one modelling approach was applied. The partial molar volume V_Φ was obtained by assuming two states for the cyclodextrin, *i.e.*, involved in the inclusion complex with a molar volume V and free in water with a molar volume V_0:

$$V_\Phi = V \cdot \frac{m_{CD-S}}{m_{CD}} + \left(1 + \frac{m_{CD-S}}{m_{CD}}\right) \cdot V_0 \qquad (6)$$

with m_{CD} and m_{CD-S} being the concentration of the free CD and of the CD involved in the inclusion complexes, obtained trough the following binding constant:

$$K = \frac{m_{CD-S}}{m_{CD} \cdot (n \cdot m_S - m_{CD-S})} \qquad (7)$$

where K is the binding constant, n is the stoichiometry, m_{CD} and m_S are the CD and surfactant molalities, respectively.

The fits are reported together with the data in Fig. 4, and the obtained fit parameters are given in the ESI† (S.3). The obtained stoichiometry values agree well with those obtained from the ITC experiments. Furthermore, high binding affinity was obtained for all the systems evaluated, and increased affinity was observed for βCD systems with ionized surfactants, whereas the opposite was found for the surfactant–αCD systems.

The volume of transfer dependence on the surfactant concentration also highlights the saturation of the cavity sites available, noticed by the constant values of ΔV^{CD} with the increase of the surfactant concentration, pointing out no further solvent displacement.

3.2 Structure of the supramolecular assemblies

One of the interesting characteristics of surfactant–CD inclusion complexes is their ability to assemble into ordered aggregates.[38] To probe these structures, small-angle scattering is an excellent technique which provides detailed insight into the organization of surfactants and CDs at the 1–100 nm scale.[21,39,40] Larger structures are well investigated using microscopy techniques.

In particular, the effect on the aggregate morphologies of the concentration, the molecular architecture of the surfactant and cyclodextrin type, and of the degree of ionization of surfactant were probed by small-angle neutron scattering. Data with mixing ratio [CD]/[S] = 2 are shown in Fig. 5.

For all the systems, macroscopically changes were observed as a function of the concentration. At 0.1 wt%, transparent fluids are obtained, while a white liquid fluid is obtained at 1% and gel aspect is observed over 3.5% for αCD systems and an increase in the birefringence and viscosity for βCD systems. The scattering profiles of those samples also point structural changes with the increase of the concentration. As shown in Fig. 5a and d, from the 0.1 to 5 wt% in the ionized surfactant complex for both surfactants, enriched microstructure is observed in more concentrated samples.

The effect of charge density is systematically probed in Fig. 5b and e for samples with 5 wt% surfactant content and mixing ratio $Y = 2$. At high charge density of the surfactant, the scattering pattern feature a $^{-2}$ power low at low-q, and

the presence of a second-order peak at a position $q_2^* = 2q_1^2$. These features are the scattering signature of periodic lamellar structures. Similar morphologies have been identified also in SDS-βCD,[41] DTAB-βCD[14] and for αCD/phytosterol ethoxylate surfactant[15] complexes. Differently, these features are not present in the curves of the nonionized surfactant complexes (Fig. 5a), indicating a lack of order in these aggregates. Similar behaviour is observed for $C_{12}E_5Ac$, with peaks slightly shifted towards lower q (Fig. 5e). The arise of order can also be noticed in the effective structure factor shown in Fig. S7 in the ESI.† In detail, the scattering profiles fully ionized $C_{12}E_{10}Ac$ present peaks at $q \approx 0.4$ and 0.82 nm^{-1} in αCD complexes and, for βCD, at $q \approx 0.6$ and 1.2 nm^{-1}, corresponding to a periodicity of 15.8 and 10.5 nm, respectively. Not only the spacing between the layers of $C_{12}E_{10}Ac$-αCD complexes is higher, but they are also more ordered, with even third-order peaks visible for $\alpha >$ 0.5. This difference can be, at least partly, ascribed to the different sizes of the CD cavities, having an outer diameter of 1.52 and 1.66 nm, corresponding to an area per molecule of 1.81 and 2.16 nm^2 for α and βCD, respectively.[40] A higher charge density in the αCD system implies stronger repulsion between the layers. Finally, the effect of the degree of ionization on later packing of the inclusion complexes is probed at high q and evidenced in the insets of Fig. 5b and e. In particular, no effect on the degree of ionization of the packing is observed for complexes formed with βCD system, while a reorganization of the structure takes place in mixtures with αCD. In the presence of the nonionized molecules, two peaks can be observed at $q \approx$ 3.45 and 5.25 nm^{-1}, with corresponding distances of 1.82 and 1.20 nm. By increasing the ionic molecules' predominance, the peaks gradually evolve to a singular signal at 4.31 nm^{-1} (Fig. 5b). We ascribe this finding to the larger spacing in the βCD system. The area per molecule of the charged $C_{12}E_{10}Ac$ at the air/water interface is 1.3 nm^2,[20] slightly less but still comparable to the area required by a αCD molecule. The effect of the type of cyclodextrin is further probed in Fig. 5c. While an effect is visible on the charged system at the higher concentration, where multilayered structures are formed, no effect is observed at a lower concentration, where the supramolecular aggregates assume a unilamellar structure.

In summary, by employing weakly acidic surfactants the effect of the charge density on the morphology of CD/S inclusion complexes could be probed. On the one hand, the presence of charges does not fundamentally affect the assembly of the inclusion complexes into bilayered structures. This is due to the relatively large spacing between the surfactant head groups. On the other hand, the gradually increasing electrostatic repulsion between the bilayers is required to provide the periodicity in the multilayered structure.

Finally, in Fig. 5f, the effect of the surfactant molecular architecture on the complexes is evidenced. For both cases, the evolution of the aggregate morphology with concentration is very similar. At high concentration, the repeating distance is smaller for $C_{12}E_5Ac$ than for $C_{12}E_{10}Ac$, with 14.8 and 10 nm for $C_{12}E_5Ac$ with αCD and βCD, respectively, and 15.8 nm for $C_{12}E_{10}Ac$-αCD and 14.1 nm for $C_{12}E_{10}Ac$-βCD system.
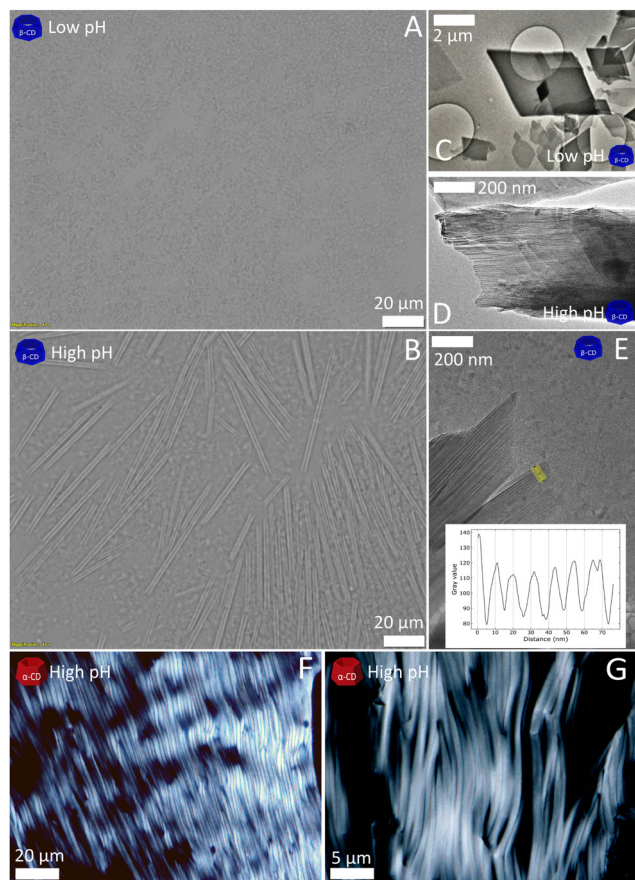
Fig. 6 Morphology of the aggregates observed for $C_{12}E_5Ac$-$2\beta CD$ inclusion complexes. Optical microscopy overview of the assemblies obtained at (a) $\alpha = 0$ and (b) $\alpha = 1$ (scale bar: 20 μm). (c) TEM picture of the rhombic structures obtained from the assembly with the nonionic surfactant (scale bar: 2 μm). (d) Cryo-TEM pictures of the tubular structure edge obtained from $\alpha = 1$ (scale bar: 200 nm) and (e) cryo-TEM picture zoom-in of the multi-layered tube wall (scale bar: 200 nm). Polarized optical microscopy images of αCD systems: (f) ionized $C_{12}E_5Ac$-αCD (scale bar: 20 μm) and (g) Ionized $C_{12}E_{10}Ac$-αCD (scale bar: 5 μm).

The lack of the Guinier domain in the SANS curves precludes the determination of the dimension and entire morphology of the assemblies. Hence, microscopic analysis was employed to unveil this aspect. The μm morphology of the inclusion complexes formed by $C_{12}E_5Ac$ with α and βCD at low and high degree of ionization is illustrated in Fig. 6. As shown in Fig. 6a, an appreciable amount of rhombic aggregates can be observed in the nonionic system. Although polydispersed in size, the crystals present the remarkable $104°$ obtuse angle characteristic of this type of cyclodextrin that can be clearly verified in the TEM image (Fig. 6c). Such structures were also reported in other βCD inclusion complexes with SDS,[12] DTAB[14] and Tween-20,[13] and it is closely related to the macrocycle symmetry. In contrast, well-defined hollow cylinders are formed in mixtures of α and βCD with the ionized surfactants (Fig. 6b, d and e for mixtures with βCD and Fig. 6f and g for mixtures with αCD). The statistical distribution of the cylinders diameters was determined from the optical microscopy image and confirms a monodispersed distribution with an average diameter equal

to 2.70 μm (standard deviation 0.24 μm) and the visible length polydispersity. However, they present distinct rigidity probed by the straightness of the tube, their positions and the absence of curvatures/bending. Cryo-EM images of a tube edge were acquired (Fig. 6e), aiming for detailed information about those structures.

Differently, for αCD systems (Fig. 6f and g), 3D network structures of long flexible fibers, often entangled, were observed. The fibers present an average diameter of 1.50 μm (standard deviation 0.25 μm) for $C_{12}E_5Ac$ (Fig. 6f), whereas slightly enlarged diameters are observed for $C_{12}E_{10}Ac$ (Fig. 6g). Although the tubular aggregates can be clearly observed for the systems with both cyclodextrins, the nature of their formation, either by the bending of the aligned layered structure[12] or by the mechanism of nucleation and growth proposed by Landman et al.,[21] could not be resolved.

4 Conclusions

This study delivers a thermodynamic and structural complementary approach of the interaction between the weakly anionic alkyl ether carboxylates and α and β-cyclodextrins. An analysis of the behaviour of the systems in aqueous solutions demonstrated the ability to spontaneously interact, forming inclusion complexes that can further self-assemble into supramolecular aggregates. The evaluation of the systems' behaviour as a function of the degree of ionization confirmed the role of the electrostatic repulsion in directing the assembly of the inclusion complexes. In this context, the present pH responsiveness of the system provided by the alkyl ethylene oxide carboxylic acids differs from the previously investigated cyclodextrin-surfactant inclusion complexes, in which only ionic or nonionic surfactants were applied mainly with β-cyclodextrin.[18,29,42] To employ a weakly acidic alkyl ether carboxylic acid, which combines the characteristics of both ionic and nonionic surfactants, allowed us the possibility to systematically change the degree of charge of the surfactant without changing the chemical nature of the guest molecule. In particular, small-angle scattering evidenced that the presence of charges is required for the spontaneous assembly of the inclusion complexes into well-ordered, multilayered structures with periodicity of ~10 nm. This long range order, arising from the electrostatic repulsion between the inclusion complex layers, can be further tuned by the CD cavity size. Finally, optical and electron microscopy revealed that the tubular structures formed with αCD are more flexible than those formed by βCD. A schematic representation of these findings is given in Fig. 7.

In contrast to the significant effect of the degree of ionization on the morphology of the supramolecular assemblies, calorimetric and densitometry results show that the complexation interaction between host and guest, is not affected by the electrostatic interactions. In addition, it hints toward the cyclodextrin binding to the alkyl chain of the surfactant rather than the ethylene oxide units of the heads, as differences in the parameters at various pH were no t observed. This seems valid even in the case of αCD, which shows a very high affinity
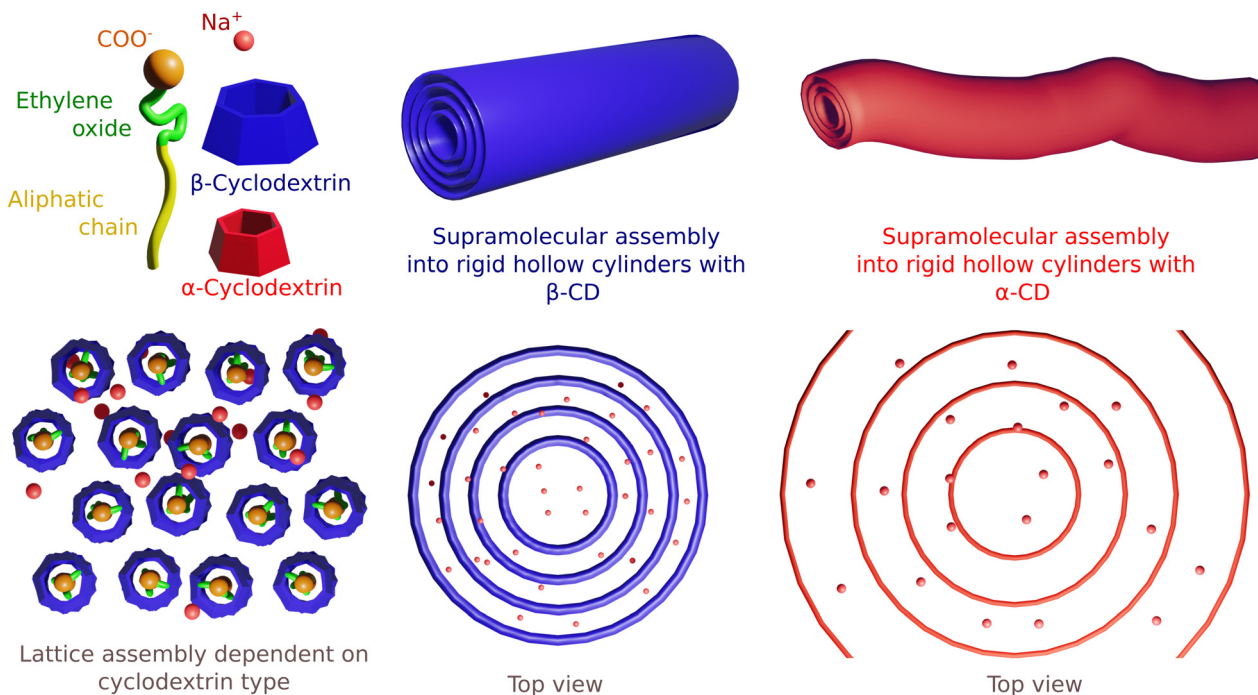
Fig. 7 Schematic representation of the components used in this work and their assembly into rigid and flexible hollow multilayered cylinders for the case of β and α cyclodextrins, respectively. The representations are not at scale and refer to the case of the fully ionized surfactant.

towards the polyethylene glycole headgroup.[10] For the latter case, a significant effect of the pH on the complexation thermodynamics was expected, as the changes in the charge density directly affects the EO units hydration state and conformation.

Controlling the electrostatic repulsion in cyclodextrin inclusion complexes systems has demonstrated to be an essential tool for not only directing the assembly, envisioning the modulation of the long-range interactions but also highlights the importance of studying the impact of the tuning parameters from the short to the long-range interactions in the hierarchical assembly process.

Conflicts of interest

There are no conflicts to declare.

Acknowledgements

References

1 A. J. Valente and O. Söderman, *Adv. Colloid Interface Sci.*, 2014, **205**, 156–176.
2 W. C. Geng, J. L. Sessler and D. S. Guo, *Chem. Soc. Rev.*, 2020, **49**, 2303–2315.
3 R. De Lisi, G. Lazzara and S. Milioto, *Phys. Chem. Chem. Phys.*, 2011, **13**, 12571–12577.
4 M. Mariano, O. D. Bernardinelli, R. Pires-Oliveira, G. A. Ferreira and W. Loh, *ACS Omega*, 2020, **5**, 9517–9528.
5 C. Perry, P. Hébraud, V. Gernigon, C. Brochon, A. Lapp, P. Lindner and G. Schlatter, *Soft Matter*, 2011, **7**, 3502–3512.
6 M. Benko and Z. Király, *J. Chem. Thermodyn.*, 2012, **54**, 211–216.
7 J. Zhang, Z. Yang, H. Zhang, Z. Hua, X. Hu, C. Liu, B. Pi and Y. Han, *Langmuir*, 2019, **35**, 16893–16899.
8 H. Dodziuk, *Cyclodextrins and Their Complexes: Chemistry, Analytical Methods, Applications*, Wiley Online Library, 2006, pp. 1–473.
9 M. Valero, I. Grillo and C. A. Dreiss, *J. Phys. Chem. B*, 2012, **116**, 1273–1281.
10 G. Lazzara, S. Prevost and M. Gradzielski, *Soft Matter*, 2011, **7**, 6082–6091.

11 J. Joseph, C. A. Dreiss, T. Cosgrove and J. S. Pedersen, *Langmuir*, 2007, **23**, 460–466.

12 S. Yang, Y. Yan, J. Huang, A. V. Petukhov, L. M. Kroon-Batenburg, M. Drechsler, C. Zhou, M. Tu, S. Granick and L. Jiang, *Nat. Commun.*, 2017, **8**, 1–7.

13 C. Zhou, X. Cheng, Q. Zhao, Y. Yan, J. Wang and J. Huang, *Langmuir*, 2013, **29**, 13175–13182.

14 J. Carlstedt, A. Bilalov, E. Krivtsova, U. Olsson and B. Lindman, *Langmuir*, 2012, **28**, 2387–2394.

15 J. Wang, W. Qi, N. Lei and X. Chen, *Colloids Surf., A*, 2019, **570**, 462–470.

16 K. Gruhle, S. Müller, A. Meister and S. Drescher, *Org. Biomol. Chem.*, 2018, **16**, 2711–2724.

17 L. Jiang, Y. Peng, Y. Yan and J. Huang, *Soft Matter*, 2011, **7**, 1726–1731.

18 L. Jiang, Y. Peng, Y. Yan, M. Deng, Y. Wang and J. Huang, *Soft Matter*, 2010, **6**, 1731–1736.

19 H. Wang, J. C. Wagner, W. Chen, C. Wang and W. Xiong, *Proc. Natl. Acad. Sci. U. S. A.*, 2020, **117**, 23385–23392.

20 L. Chiappisi, *Adv. Colloid Interface Sci.*, 2017, **250**, 79–94.

21 J. Landman, S. Ouhajji, S. Prévost, T. Narayanan, J. Groenewold, A. P. Philipse, W. K. Kegel and A. V. Petukhov, *Sci. Adv.*, 2018, **4**, 1–8.

22 D. W. Hayward, L. Chiappisi, J. H. Teo, S. Prévost, R. Schweins and M. Gradzielski, *Soft Matter*, 2019, **15**, 8611–8620.

23 L. Chiappisi, I. Hoffmann and M. Gradzielski, *Soft Matter*, 2013, **9**, 3896–3909.

24 J. Hernandez-Pascacio, A. Pineiro, J. M. Ruso, N. Hassan, R. A. Campbell, J. Campos-Terán and M. Costas, *Langmuir*, 2016, **32**, 6682–6690.

25 P. Lindner and R. Schweins, *Neutron News*, 2010, **21**, 15–18.

26 Laue-Langevin, *D22 – Large dynamic range smallangle diffractometer*, Institut Laue-Langevin, 2003, https://www.ill. eu/users/instruments/instrumentslist/d22/description/ instrument-layout.

27 W. Saenger and T. Steiner, *Acta Crystallogr., Sect. A: Found. Crystallogr.*, 1998, **A54**, 798–805.

28 L. E. Briggner and I. Wadsö, *J. Chem. Thermodyn.*, 1990, **22**, 1067–1074.

29 D. Ondo, *J. Mol. Liq.*, 2020, **311**, 113172.

30 I. Araujo Marques, A. J. Patino-Agudelo, Y. L. Coelho, P. D. Santos Moreau, L. Neves Santa Rosa, A. C. dos Santos Pires and L. H. Mendes da Silva, *J. Mol. Liq.*, 2021, **338**, 116647.

31 B. K. Müller and H. Ritter, *J. Inclusion Phenom. Macrocyclic Chem.*, 2012, **72**, 157–164.

32 L. Liu and Q. X. Guo, *J. Inclusion Phenom.*, 2002, **42**, 1–14.

33 R. De Lisi, G. Lazzara, S. Milioto and N. Muratore, *J. Phys. Chem. B*, 2003, **107**, 13150–13157.

34 I. V. Terekhova, R. De Lisi, G. Lazzara, S. Milioto and N. Muratore, *J. Therm. Anal. Calorim.*, 2008, **92**, 285–290.

35 K. Spildo and H. Høiland, *J. Solution Chem.*, 2002, **31**, 149–164.

36 M. Manabe, T. Ochi, H. Kawamura, H. Katsu-Ura, M. Shiomi and M. S. Bakshi, *Colloid Polym. Sci.*, 2005, **283**, 738–746.

37 L. D. Wilson and R. E. Verrall, *J. Phys. Chem. B*, 1997, **101**, 9270–9279.

38 K. Liu, C. Ma, T. Wu, W. Qi, Y. Yan and J. Huang, *Curr. Opin. Colloid Interface Sci.*, 2020, **45**, 44–56.

39 S. Ouhajji, J. Landman, S. Prévost, L. Jiang, A. P. Philipse and A. V. Petukhov, *Soft Matter*, 2017, **13**, 2421–2425.

40 L. dos Santos Silva Araújo, G. Lazzara and L. Chiappisi, *Adv. Colloid Interface Sci.*, 2021, **289**, 102375.

41 L. Jiang, Y. Yan and J. Huang, *Adv. Colloid Interface Sci.*, 2011, **169**, 13–25.

42 A. Mahata, D. Bose, D. Ghosh, B. Jana, B. Bhattacharya, D. Sarkar and N. Chattopadhyay, *J. Colloid Interface Sci.*, 2010, **347**, 252–259.